

Short note

Isotropic discrete Laplacian operators from lattice hydrodynamics

Sumesh P. Thampi^{a,*}, Santosh Ansumali^a, R. Adhikari^b, Sauro Succi^c^a Engineering Mechanics Unit, Jawaharlal Nehru Centre for Advanced Scientific Research, Bangalore 560064, India^b The Institute of Mathematical Sciences, CIT Campus, Chennai 600113, India^c Istituto Applicazioni Calcolo, CNR Roma – via dei Taurini 9, 00185 Roma, Italy

ARTICLE INFO

Article history:

Received 16 February 2012

Received in revised form 12 July 2012

Accepted 24 July 2012

Available online 14 August 2012

Keywords:

Isotropic Laplacians

Lattice hydrodynamics

ABSTRACT

We show that discrete schemes developed for lattice hydrodynamics provide an elegant and physically transparent way of deriving Laplacians with isotropic discretisation error. Isotropy is guaranteed whenever the Laplacian weights follow from the discrete Maxwell–Boltzmann equilibrium since these are, by construction, isotropic on the lattice. We also point out that stencils using as few as 15 points in three dimensions, generate isotropic Laplacians. These computationally efficient Laplacians can be used in cell-dynamical and hybrid lattice Boltzmann simulations, in favor of popular anisotropic Laplacians, which make use of larger stencils. The method can be extended to provide discretisations of higher order and for other differential operators, such the gradient, divergence and curl.

© 2012 Elsevier Inc. All rights reserved.

1. Introduction

Isotropy, an essential property of the Laplacian operator, is a desirable feature in any of its discrete representations. However, most commonly used discretisations of the Laplacian suffer from error terms that are anisotropic. These infect numerical solutions with anisotropies when, in fact, physical solutions are required to be isotropic. Two recent studies have addressed this issue, by providing algebraic methods for constructing isotropic Laplacians [1,2]. In this paper, we show that lattices and associated weights used in lattice hydrodynamic simulations, naturally provide discrete Laplacians with isotropic discretisation error. These lattices and weights have been known for a long time in the lattice Boltzmann literature [3,4], but their connection to isotropic Laplacians has not been recognized. Though some previous studies [5] have proposed schemes based on lattice Boltzmann to solve diffusion equations, here, we make this connection explicit and also show how discretisations of other differential operators like the gradient and divergence follow from it.

Below, we first provide our main results for the isotropically discretised Laplacian. We then provide a derivation of our result and make explicit its connection with the discrete Maxwell–Boltzmann equilibrium on the lattice. We conclude with a comparison of the isotropy properties of our Laplacians with those proposed earlier.

Consider the cubic cell in Fig. 1 with center e_0 , the 6 vectors \mathbf{c}_i^1 that point to the face centers e_1 , the 12 vectors \mathbf{c}_i^2 that point to the edge centers e_2 and the 8 vectors \mathbf{c}_i^3 that point to the vertices e_3 . The face center vectors point along the Cartesian axes and so have the form $(\pm 1, 0, 0)$ with two vanishing Cartesian components, the edge center vectors are confined to the Cartesian planes and so have form $(\pm 1, \pm 1, 0)$ with one vanishing Cartesian component, while the vertex vectors have the form $(\pm 1, \pm 1, \pm 1)$. (With this choice, the discretisation step is set to unity.) This suggests an “energy shell” classification, where the energy is identified with the squared modulus of the vector. Then, the 27 points of the cubic cell lie on the “energy shells” with energies $e_j = 0, 1, 2, 3$. There is 1 null vector \mathbf{c}^0 on the energy shell $e = 0$, 6 vectors \mathbf{c}_i^1 on the energy shell $e = 1$, 12 vectors \mathbf{c}_i^2 on the energy shell $e = 2$ and 8 vectors \mathbf{c}_i^3 on the energy shell $e = 3$. In the cell dynamics literature these are known as the nearest neighbors – NN, next nearest neighbors – NNN, and next next nearest neighbors – NNNN, respectively.

* Corresponding author.

E-mail address: sumesh.pt@gmail.com (S.P. Thampi).

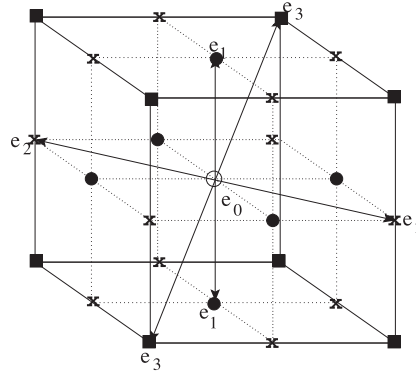


Fig. 1. Ordering of points on a cubic unit cell according to “energy shells”, as explained in the text. Here e_0, e_1, e_2, e_3 represent the energy shells corresponding to $e = 0, 1, 2, 3$, marked by \circ, \bullet, \times and \blacksquare respectively. For clarity, only one pair is highlighted.

For a function $\psi(\mathbf{r})$ defined on such a cubic grid, we use the convenient shorthand $\psi(\mathbf{r} + \mathbf{c}_i^j) = \psi_i^{(j)}$ for its value on the i th point of the j th energy shell. Then, our main results for the isotropic Laplacian $L(\mathbf{r}) \equiv \nabla^2 \psi(\mathbf{r})$ are

$$L(\mathbf{r})_{D2Q9} = \frac{1}{6} \left[4 \sum_{i=1}^4 \psi_i^{(1)} + \sum_{i=1}^4 \psi_i^{(2)} - 20\psi^{(0)} \right] \quad (1)$$

$$L(\mathbf{r})_{D3Q19} = \frac{1}{6} \left[2 \sum_{i=1}^6 \psi_i^{(1)} + \sum_{i=1}^{12} \psi_i^{(2)} - 24\psi^{(0)} \right] \quad (2)$$

$$L(\mathbf{r})_{D3Q15} = \frac{1}{12} \left[8 \sum_{i=1}^6 \psi_i^{(1)} + \sum_{i=1}^8 \psi_i^{(3)} - 56\psi^{(0)} \right] \quad (3)$$

$$L(\mathbf{r})_{D3Q27} = \frac{1}{36} \left[16 \sum_{i=1}^6 \psi_i^{(1)} + 4 \sum_{i=1}^{12} \psi_i^{(2)} + \sum_{i=1}^8 \psi_i^{(3)} - 152\psi^{(0)} \right] \quad (4)$$

The first of these is a two-dimensional Laplacian which uses the 4 face centers and 4 edge centers on a Cartesian plane, while the remaining are all three dimensional Laplacians. The subscript on each of these Laplacians indicates that they derive from a $DnQm$ lattice hydrodynamic model, as we explain in detail below.

2. Laplacians from lattice equilibria

The lattice formulation of kinetic theory provides a computationally efficient algorithm for solving the Navier–Stokes and related equations [4]. A central quantity in lattice kinetic theory is the discrete form of the Maxwell–Boltzmann velocity distribution. There are several routes by which these equilibria can be obtained [6,7]. Here, we focus on the lattice generalization of the earliest derivation by Maxwell [6], which appeals only to factorisability and isotropy. Briefly, Maxwell argued that the distribution function $f(\mathbf{c})$ must be isotropic in velocity space and so must be function of $c^2 = \mathbf{c} \cdot \mathbf{c}$ and it must be factorisable so that $f(\mathbf{c}) = f(c_x)f(c_y)f(c_z)$. The only function that satisfies both these requirements is the Gaussian $f(\mathbf{c}) \sim \exp(-c^2/2k_B T)$, whose variance $k_B T$ is fixed by requiring consistency with thermodynamics, and whose prefactor is fixed by normalization. In the above, the mass has been set to unity. Recent works [8,9] show that a cubic lattice containing 27 velocities, made out of the direct product of the velocity set $\{-1, 0, 1\}$, has both the isotropy and factorisability features required by the continuum Maxwellian. This provides a succinct derivation of the lattice Maxwellian. The 27 velocity lattice and the weights so generated are called D3Q27 in the lattice hydrodynamics literature. Projections of this lattice to smaller velocity set are possible. In such projections, factorisability is lost, but isotropy is still maintained. It is well-known that isotropy of the lattice Maxwellians is a necessary condition for Navier–Stokes hydrodynamics on the lattice. It is this feature that we exploit to generate the isotropic Laplacians listed above.

We begin with a $DnQm$ lattice hydrodynamic model in n dimensions with m velocities. These have discrete weights w_i^j which correspond to the energy shells e_j . For a scalar function $\psi(\mathbf{r})$ defined on such a lattice, consider the transform

$$\langle \psi(\mathbf{r}) \rangle = \sum_{j=0}^3 \sum_{i=1}^{N_j} w_i^j \psi(\mathbf{r} + \mathbf{c}_i^j) \quad (5)$$

where i labels the i th discrete velocity in the j th energy shell with N_j velocities and w_i^j is the corresponding weight factor. As is well known, the necessary conditions for obtaining isotropic Navier–Stokes hydrodynamics on the lattice are [10]

$$\sum_{ij} w_i^j = 1 \quad (6)$$

$$\sum_{ij} w_i^j c_{i,\alpha}^j c_{i,\beta}^j = T \delta_{\alpha\beta} \quad (7)$$

$$\sum_{ij} w_i^j c_{i,\alpha}^j c_{i,\beta}^j c_{i,\gamma}^j c_{i,\lambda}^j = T^2 \Delta_{\alpha\beta\gamma\lambda}^{(4)} \quad (8)$$

where Greek indices label Cartesian directions and $\Delta_{\alpha\beta\gamma\lambda}^{(4)} = \delta_{\alpha\beta}\delta_{\gamma\lambda} + \delta_{\alpha\lambda}\delta_{\gamma\beta} + \delta_{\alpha\gamma}\delta_{\beta\lambda}$. It may be noted that expressions containing odd powers of \mathbf{c} vanish. In the above T is a lattice-dependent constant which identifies with the temperature of the moving particles. Using particles in the cubic cell with velocities $c_{i,\alpha} = \{-1, 0, 1\}$, the identity $c_{i,\alpha}^2 = c_{i,\alpha}^4$ implies $T = 1/3$ as the only value ensuring isotropy of the lattice hydrodynamics in the cubic cell. All weighted polynomials odd in the velocities vanish identically. In particular, linear, cubic and quintic polynomials are zero. On these lattices, the sextic polynomials are the first non-zero polynomials to break isotropy.

Taylor expanding $\psi(\mathbf{r} + \mathbf{c}_i^j)$ in Eq. (5) and applying the above symmetries of Eqs. (6)–(8), we obtain

$$\langle \psi(\mathbf{r}) \rangle = \psi(\mathbf{r}) + \frac{T}{2} \nabla^2 \psi(\mathbf{r}) + \frac{T^2}{8} \nabla^4 \psi(\mathbf{r}) + O(\nabla^6) \quad (9)$$

This equation can be solved for Laplacian $L(\mathbf{r}) \equiv \nabla^2 \psi(\mathbf{r})$ to obtain

$$L(\mathbf{r}) = \frac{2}{T} \left[\sum_{j=0}^3 \sum_{i=1}^{N_j} w_i^j \psi(\mathbf{r} + \mathbf{c}_i^j) - \psi(\mathbf{r}) \right] + O(\nabla^4) \quad (10)$$

This automatically secures isotropy of the Laplacian up to leading order error, with an error coefficient of order $O(T)$. This error cannot be made zero with the given cubic stencil. The above expression is remarkable, because any lattice with suitable weights which satisfies the conditions in Eqs. (6)–(8) will provide an expression for the discrete Laplacian operator and will ensure isotropy. Writing down the terms of Eq. (10) explicitly, with $\psi_i^{(j)}$ for $\psi(\mathbf{r} + \mathbf{c}_i^j)$, we have

$$L(\mathbf{r}) = \frac{2}{T} \left[\sum_{i=1}^6 w_i^1 \psi^{(1)} + \sum_{i=1}^{12} w_i^2 \psi^{(2)} + \sum_{i=1}^8 w_i^3 \psi^{(3)} + (w^0 - 1) \psi^{(0)} \right] \quad (11)$$

In other words, by redefining $\hat{w}^0 = w^0 - 1$ and $\hat{w}^j = w^j$ for $j = 1, 2, 3$ we have

$$\sum_{ij} \hat{w}_i^j = 0 \quad (12)$$

to replace Eq. (6) which, along with Eqs. 7 and 8, form a set of weights, $\{\hat{w}\}$, required to construct isotropic Laplacian operators in discrete space. These weights are lattice analogues of Hermite weights related to the Maxwell–Boltzmann equilibrium. Hence, this method of deriving isotropic Laplacians is an elegant and physically transparent way of calculating the operators compared to the methods present in the literature [1,2].

This general expression, when applied to the D2Q9, D3Q15, D3Q19, D3Q27 models, whose weights are listed in Table 1, gives the isotropic Laplacians we listed previously. Models with different number of energy shells may also be chosen. The two-dimensional D2Q9 Laplacian was obtained earlier by a different argument in [1]. Interestingly, isotropic three-dimensional Laplacians can be achieved with just 15 or 19 velocities, i.e. in D3Q15 and D3Q19 using Eq. (10), and it is not necessary to use all 27 velocities. This result was obtained earlier [11,12], with weights identical to D3Q15 and D3Q19, without realizing the connection with lattice hydrodynamics.

3. Discussion

Having derived the Laplacians, we next proceed to compare their isotropy properties with other commonly used Laplacians, listed below.

Table 1

Energy shells and the corresponding weight factors for various DnQm lattice hydrodynamics models. Values of N_j for the two dimensional model D2Q9 are given in brackets.

e^j	N_j , (for 2D)	w_i^j	D2Q9	D3Q15	D3Q19	D3Q27
0	1 (1)	w_i^0	4/9	2/9	1/3	8/27
1	6 (4)	w_i^1	1/9	1/9	1/18	2/27
2	12 (4)	w_i^2	1/36	0	1/36	1/54
3	8 (0)	w_i^3	0	1/72	0	1/216

$$L(\mathbf{r})_{CD} = \sum_{i=1}^6 \psi_i^{(1)} - 6\psi^{(0)} \quad (13)$$

$$L(\mathbf{r})_{PK} = \frac{1}{30} \left(14 \sum_{i=1}^6 \psi_i^{(1)} + 3 \sum_{i=1}^{12} \psi_i^{(2)} + \sum_{i=1}^8 \psi_i^{(3)} - 128\psi^{(0)} \right) \quad (14)$$

$$L(\mathbf{r})_{SO} = \frac{1}{22} \left(6 \sum_{i=1}^6 \psi_i^{(1)} + 3 \sum_{i=1}^{12} \psi_i^{(2)} + \sum_{i=1}^8 \psi_i^{(3)} - 80\psi^{(0)} \right) \quad (15)$$

$$L(\mathbf{r})_{KU} = \frac{1}{48} \left(20 \sum_{i=1}^6 \psi_i^{(1)} + 6 \sum_{i=1}^{12} \psi_i^{(2)} + \sum_{i=1}^8 \psi_i^{(3)} - 200\psi^{(0)} \right) \quad (16)$$

$$L(\mathbf{r})_{EW} = \frac{1}{9} \left(\sum_{i=1}^6 \psi_i^{(1)} + \sum_{i=1}^{12} \psi_i^{(2)} + \sum_{i=1}^8 \psi_i^{(3)} - 26\psi^{(0)} \right) \quad (17)$$

The suffixes *CD*, *PK*, *SO*, *KU*, *EW* stand for central difference, Patra–Kartunnen, Shinozaki–Oono, Kumar and ‘equally weighted’ respectively. Eq. (13) is the standard central finite-difference expression. Eq. (14) has been systematically derived by imposing conditions of rotational invariance and isotropy of the operator [2,13]. Eq. (15) is popular in the cell-dynamics and phase separation studies [14]. Eq. (16) has been introduced as part of isotropic finite differences which describes discrete derivative operations without directional bias [1]. Eq. (17) is a simple expression used in lattice Boltzmann simulations [15,16] which gives equal weightage to all energy shells. In the small wave number limit, the discrete Fourier transform $L(\mathbf{k}) = \sum_{\mathbf{r}} \exp(-i\mathbf{k} \cdot \mathbf{r}) L(\mathbf{r}) / \sum_{\mathbf{r}} \exp(-i\mathbf{k} \cdot \mathbf{r}) \psi(\mathbf{r})$ of the Laplacian operator corresponding to the above expressions (Eqs. (2)–(4), (13)–(17)) can be written as

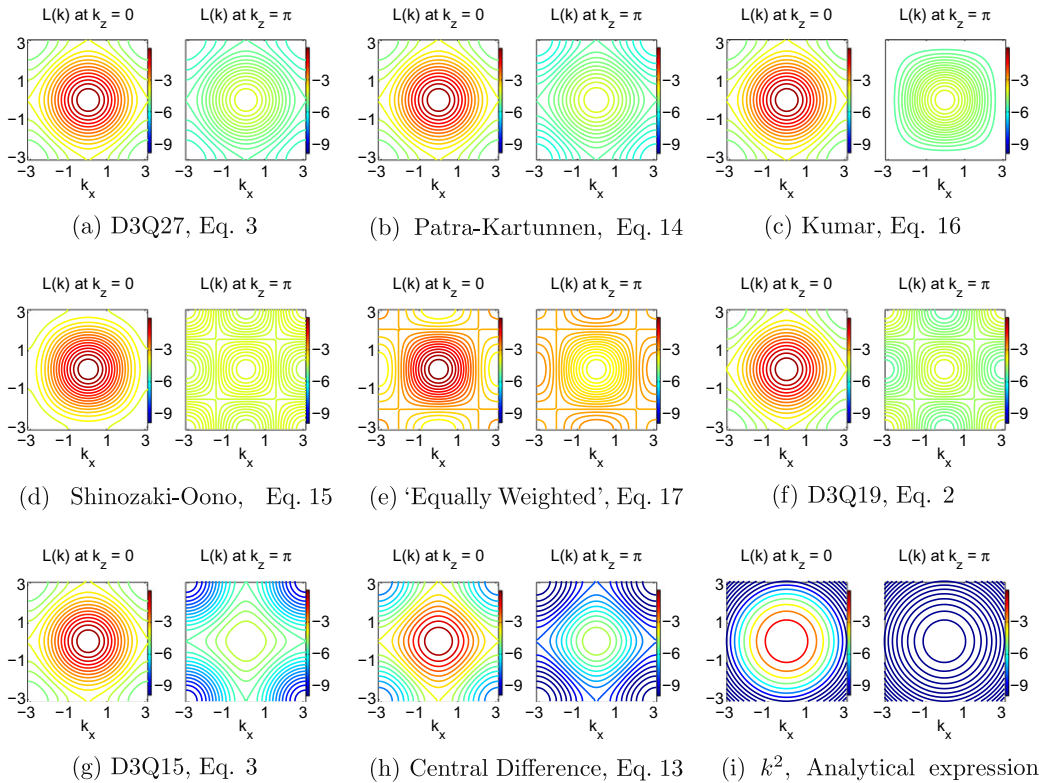


Fig. 2. Isocontours of the Laplacian operators in Fourier space, $L(\mathbf{k})$, at two different planes at $k_z = 0$ and $k_z = \pi$. Also shown is the isotropic plot of k^2 at these two planes for comparison. The color-bar is kept same for comparison across the operators. The y-axis is shown only for the first plot among each set for clarity.

$$L(\mathbf{k})_{D3Q15} = -k^2 + \frac{k^4}{12} + O(k_\alpha^6) \quad (18)$$

$$L(\mathbf{k})_{D3Q19} = -k^2 + \frac{k^4}{12} + O(k_\alpha^6) \quad (19)$$

$$L(\mathbf{k})_{D3Q27} = -k^2 + \frac{k^4}{12} + O(k_\alpha^6) \quad (20)$$

$$L(\mathbf{k})_{CD} = -k^2 + \left[\frac{k^4}{12} - \frac{k_x^2 k_y^2 + k_x^2 k_z^2 + k_y^2 k_z^2}{6} \right] + O(k_\alpha^6) \quad (21)$$

$$L(\mathbf{k})_{PK} = -k^2 + \frac{k^4}{12} + O(k_\alpha^6) \quad (22)$$

$$L(\mathbf{k})_{SO} = -k^2 + \left[\frac{k^4}{12} + \frac{k_x^2 k_y^2 + k_x^2 k_z^2 + k_y^2 k_z^2}{33/2} \right] + O(k_\alpha^6) \quad (23)$$

$$L(\mathbf{k})_{KU} = -k^2 + \frac{k^4}{12} + O(k_\alpha^6) \quad (24)$$

$$L(\mathbf{k})_{EW} = -k^2 + \left[\frac{k^4}{12} + \frac{k_x^2 k_y^2 + k_x^2 k_z^2 + k_y^2 k_z^2}{6} \right] + O(k_\alpha^6) \quad (25)$$

Isotropy at fourth order in k is observed for all $DnQm$ lattice stencils. This is also true for PK and KU stencils. Other stencils show anisotropic discretisation errors. While one may expect Eq. (13) to be anisotropic, due to the simplicity in construction, Eqs. (15) and (17) use all 27 points of the cubic cell, but are still not isotropic at leading order in error. None of these stencils provides isotropic error at sixth order.

In Fig. 2, we plot isocontours of the Laplacian in Fourier space along the planes $k_z = 0, \pi$, to visually represent the degrees of anisotropy beyond quartic order. Fig. 3 has the corresponding error plots. Both $D3Q27$ and Patra–Kartunnen Laplacians exhibit similar behavior and are the best of the set. The Laplacian introduced by Kumar also exhibits comparable behavior. Both Shinozaki–Oono and ‘equally weighted’ Laplacians are poor approximations at large wavenumbers and as seen from Eqs. (15)–(17) they are not isotropic at quartic order. Both $D3Q19$ and $D3Q15$ are isotropic at quartic order with smaller

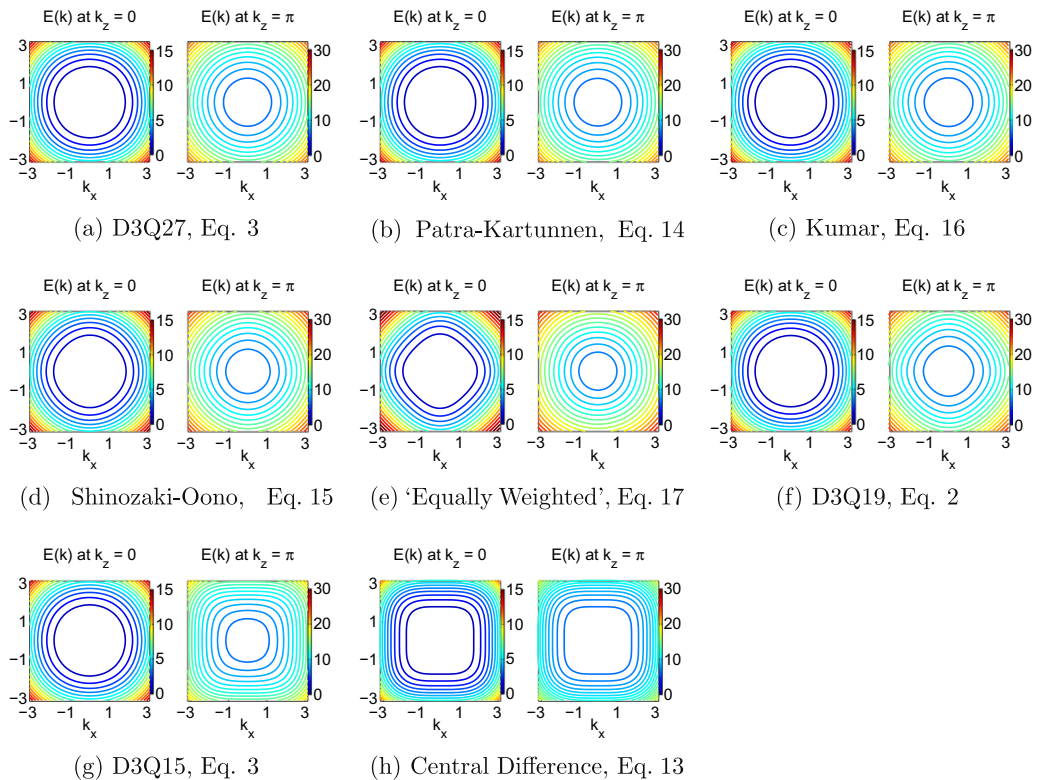


Fig. 3. Isocontours of the error of Laplacian operators in Fourier space defined as $E(\mathbf{k}) = |L(\mathbf{k}) - (-k^2)|$ at two different planes at $k_z = 0$ and $k_z = \pi$ (same as in Fig. 2). The color-bar is kept same for comparison across the operators. The y-axis is shown only for the first among each set for clarity.

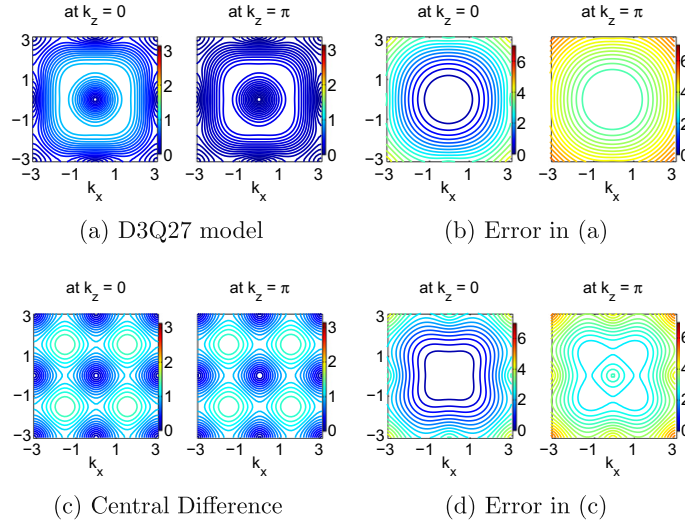


Fig. 4. Isocontours of the Gradient operators and the errors in Fourier space at two different planes at $k_z = 0$ and $k_z = \pi$. Note that the form of the operators remain same for divergence and curl operators.

stencils consisting of 19 and 15 points. The smallest of central difference stencil is the most anisotropic of the set, as seen in Fig. 2(h). Laplacians which have identical isotropic errors at quartic order may still have different stability properties when employed in numerical algorithms. This is part of ongoing work, and will be reported elsewhere.

Our method naturally generalizes to other differential operators as well. Here, we provide a brief description of these operators. Let us consider the transform

$$\langle \psi(\mathbf{r}) \rangle = \sum_{j=0}^3 \sum_{i=1}^{N_j} w_i^j \mathbf{c}_i^j \psi(\mathbf{r} + \mathbf{c}_i^j) \quad (26)$$

Upon Taylor expanding $\psi(\mathbf{r} + \mathbf{c}_i^j)$ in Eq. (26) and using the symmetries of Eqs. (6)–(8), we obtain the gradient operator. Appropriately modifying the operation between \mathbf{c} and a vector field $\psi(\mathbf{r})$, both divergence and curl can also be obtained. To leading order, these read as follows, respectively:

$$\nabla \psi = \frac{1}{T} \sum_{j=0}^3 \sum_{i=1}^{N_j} w_i^j \mathbf{c}_i^j \psi(\mathbf{r} + \mathbf{c}_i^j) + O(\nabla^3) \quad (27)$$

$$\nabla \cdot \psi = \frac{1}{T} \sum_{j=0}^3 \sum_{i=1}^{N_j} w_i^j \mathbf{c}_i^j \cdot \psi(\mathbf{r} + \mathbf{c}_i^j) + O(\nabla^3) \quad (28)$$

$$\nabla \wedge \psi = \frac{1}{T} \sum_{j=0}^3 \sum_{i=1}^{N_j} w_i^j \mathbf{c}_i^j \wedge \psi(\mathbf{r} + \mathbf{c}_i^j) + O(\nabla^3). \quad (29)$$

This automatically secures isotropy of the operators up to leading order error. Isocontour lines of the gradient operator and the error for a D3Q27 model are shown in Fig. 4. For comparison, the results obtained with a central difference operator are also shown.

A systematic account of gradient, divergence and curl operators obtained by this method, as well as the case of genuine anisotropic physics [17], and higher order lattices [18,19], will be reported elsewhere.

4. Summary and outlook

Summarizing, we have shown that lattices and weights commonly employed in lattice hydrodynamic simulations, provide a computationally efficient discrete representation of the Laplacian preserving isotropy up to leading order error. The weights are derived from the lattice analogue of the Maxwell–Boltzmann distribution and are related to Hermite series expansion of local Maxwell–Boltzmann distributions. The use of these Laplacians should prove beneficial for cell dynamics simulations, hybrid lattice Boltzmann simulations, and many other problems, where efficient isotropic discretizations of the Laplacian are required.

Acknowledgements

One of the authors (SS) wishes to thank the Indian Academy of Sciences for financial support and kind hospitality. ST and SA acknowledge the discussions with Rashmi Ramadugu.

References

- [1] A. Kumar, J. Comput. Phys. 201 (2004) 109–118.
- [2] M. Patra, M. Karttunen, Numer. Methods Part. Differ. Equat. 22 (2005) 936–953.
- [3] Y.H. Qian, D. D’Humières, P. Lallemand, Europhys. Lett. 17 (1992) 479–484.
- [4] (a) R. Benzi, S. Succi, M. Vergassola, Phys. Rep. 222 (1992) 145;
(b) C. Aidun, Y. Lu, Ann. Rev. Fluid Mech. 42 (2010) 439.
- [5] R.G.M. van der Sman, Phys. Rev. E 74 (2006) 026705.
- [6] J.C. Maxwell, Philos. Mag. Ser. 4 19 (1860) 19–32.
- [7] L. Boltzmann, Wien. Ber. 66 (1871) 275–370.
- [8] S. Ansumali, I.V. Karlin, H.C. Ottinger, Europhys. Lett. 63 (2003) 798–804.
- [9] I. Karlin, P. Asinari, Physica A 8 (2010) 1530–1548.
- [10] H. Chen, I. Goldhirsch, S.A. Orszag, J. Sci. Comput. 34 (2008) 87–112.
- [11] M.M. Gupta, J. Kouatchou, Numer. Methods Part. Differ. Equat. 14 (1998) 593–606.
- [12] U. Ananthakrishnaiah, R.P. Manohar, J.W. Stephenson, Numer. Methods Part. Differ. Equat. 3 (1987) 229–240.
- [13] W.F. Spatz, G.F. Carey, Numer. Methods Part. Differ. Equat. 12 (1996) 235–243.
- [14] A. Shinozaki, Y. Oono, Phys. Rev. E. 48 (1993) 2622–2654.
- [15] V.M. Kendon, M.E. Cates, I. Pagonabarraga, J.C. Desplat, P. Bladon, J. Fluid, Mech. 440 (2001) 147–203.
- [16] J.C. Desplat, I. Pagonabarraga, P. Bladon, Comput. Phys. Commun. 134 (2001) 273–290.
- [17] I. Rasin, W. Miller, S. Succi, J. Comput. Phys. 206 (2005) 453–462.
- [18] M. Sbragaglia, R. Benzi, L. Biferale, S. Succi, K. Sugiyama, F. Toschi, Phys. Rev. E 75 (2007) 026702.
- [19] X. Shan, Phys. Rev. E 77 (2008) 066702.